# Effect of Tesla valve geometry on unsteady flow behavior and pressure drop - A CFD study

## *Efecto de la geometría de la válvula Tesla en el comportamiento del flujo inestable y la caída de presión: un estudio de CFD*

## *Efeito da geometria da válvula Tesla no comportamento do fluxo instável e na queda de pressão - Um estudo de CFD*

*Muhammad Shakaib [1(*)], Muhammad Ehtesham ul Haque [2], Syed Muhammad Fakhir Hasani [3]*

Recibido: 08/04/2025 Aceptado: 23/07/2025

**Summary. -** Computational fluid dynamics (CFD) simulations are carried out to examine the effect of geometric parameters of Tesla valve on flow patterns, pressure drop and flow diodicity. In forward flow, the flow is relatively smooth with less flow resistance. The low velocity regions are present at the entrance to the curved section and at the junction of the curved section and the exit channel, where flow separation takes place. In reverse flow, the flow is quite irregular, and major recirculation zones are observed in the bottom branch, in addition to the top-curved and exit sections. The simulations with small time steps show that the flow is steady when the flow takes place in the forward direction. The flow is mostly transient; however, when the fluid flows in the reverse direction, particularly at higher Reynolds numbers. The effect of geometric parameters such as the angles subtended by the curved section (with the horizontal) shows that optimal values of these angles exist. For a certain range of angles, diodicity is greater than 2. The effect of multi-staging of the Tesla valve is studied, and it is found that the flow unsteadiness and overall diodicity increase with the number of stages.

***Keywords:*** Micro/Nano Fluidics, Tesla Valve, Computational Fluid Dynamics, Pressure drop, Diodicity.

[1] Professor, Department of Mechanical Engineering, NED University of Engineering and Technology (Pakistan), mshakaib@neduet.edu.pk, ORCID iD: https://orcid.org/0000-0003-0699-1987

[2] Assistant Professor, Department of Mechanical Engineering, NED University of Engineering and Technology (Pakistan), mehaque@neduet.edu.pk, ORCID iD: https://orcid.org/0000-0001-8751-348X

[3] Associate Professor, Department of Mechanical Engineering, Imam Mohammad Ibn Saud Islamic University (Saudi Arabia), smhasani@imamu.edu.sa, ORCID iD: https://orcid.org/0000-0002-6202-1996

Memoria Investigaciones en Ingeniería, núm. 29 (2025). pp. 54-73
https://doi.org/10.36561/ING.29.5
ISSN 2301-1092 • ISSN (en línea) 2301-1106 – Universidad de Montevideo, Uruguay

***Resumen. -*** *Simulaciones de dinámica de fluidos computacional (CFD) fueron realizadas para examinar el efecto de los parámetros geométricos de la válvula Tesla en los patrones de flujo, la caída de presión y la diodicidad del flujo. En flujo directo, el flujo es relativamente suave y presenta poca resistencia. Se observan regiones de baja velocidad en la entrada de la sección curva y en la unión de esta con el canal de salida, donde se produce la separación del flujo. En flujo inverso, el flujo es bastante irregular y se observan importantes zonas de recirculación en la rama inferior, además de en las secciones superior curva y de salida. Las simulaciones con pasos de tiempo pequeños muestran que el flujo es estacionario en la dirección directa. Sin embargo, el flujo es mayormente transitorio en la dirección inversa, particularmente a números de Reynolds elevados. El efecto de parámetros geométricos como los ángulos subtendidos por la sección curva (con respecto a la horizontal) muestra que existen valores óptimos para estos ángulos. Para un cierto rango de ángulos, la diodicidad es mayor que 2. Se estudia el efecto de la multietapa de la válvula Tesla y se encuentra que la inestabilidad del flujo y la diodicidad general aumentan con el número de etapas.*

***Palabras clave:*** *Microfluídica/nanofluídica, válvula Tesla, dinámica de fluidos computacional, caída de presión, diodicidad.*

***Resumo***. ***-*** *Simulações de dinâmica dos fluidos computacional (CFD) foram realizadas para examinar o efeito dos parâmetros geométricos da válvula Tesla nos padrões de fluxo, na queda de pressão e na diodicidade do fluxo. No fluxo direto, o fluxo é relativamente suave, com menor resistência. Regiões de baixa velocidade estão presentes na entrada da seção curva e na junção da seção curva com o canal de saída, onde ocorre a separação do fluxo. No fluxo reverso, o fluxo é bastante irregular e grandes zonas de recirculação são observadas no ramo inferior, além das seções curvas superiores e de saída. As simulações com pequenos passos de tempo mostram que o fluxo é estável quando ocorre na direção direta. O fluxo é predominantemente transiente quando o fluido flui na direção reversa, particularmente em números de Reynolds mais altos. O efeito de parâmetros geométricos, como os ângulos subtendidos pela seção curva (com a horizontal), mostra que existem valores ótimos para esses ângulos. Para uma determinada faixa de ângulos, a diodicidade é maior que 2. O efeito do funcionamento em múltiplos estágios da válvula Tesla é estudado, e constata-se que a instabilidade do fluxo e a diodicidade geral aumentam com o número de estágios.*

***Palavras-chave:*** *Micro/Nanofluidos, Válvula Tesla, Dinâmica dos Fluidos Computacional, Queda de pressão, Diodicidade.*

**1. Introduction. -** A non-return valve (NRV) is a common device in piping systems that allows the fluid to flow in one direction while restricting its flow in the opposite direction. The 'one-way' operation of the valve in these systems may be necessary for various reasons, such as safe operation of the mechanical equipment, avoiding mixing or contamination of fluid streams or in general to ensure desired system performance. Many of the NRVs utilize a ball/poppet with a seat and spring arrangement. The ball moves in a particular direction due to fluid force, allowing the fluid flow in one direction while blocking it in the opposite direction. Another type of non-return valve is the Tesla valve, which, because of its geometrical design, offers more resistance when fluid flows in the reverse direction compared to its forward movement. It does not require any manual or electronic operation, and unlike other NRV types, it does not have any internal moving element to open or close the flow passage. Invented more than a century ago by Nikola Tesla (1920), its use has reemerged in recent times due to its potential application in microfluidic devices. Tesla valves have been found useful in applications where low flow rates are required or in situations where moving parts can cause a significant reduction in the overall efficiency of the device. The Tesla valve behaves much like a diode in electronics, which allows the current to flow only in one direction and blocks the current flow in the opposite direction. Like a diode, the Tesla valve offers higher flow resistance due to its complex geometry, creating vortex-type flow structures as it flows in one direction and offers much less resistance when its flow direction is reversed. This feature of the Tesla valve is defined in terms of its diodicity, which is the ratio of the pressure drop in the reverse direction to the pressure drop in the forward direction. The pressure drop in forward/reverse direction or diodicity depends on the geometrical characteristics of the Tesla valve, the fluid properties and the flow velocities. The resurfacing of the Tesla valve technology in modern-day micro and nano fluidics has been discussed in detail in a historical review paper by Purwidyantri and Prabowo (2023). A comprehensive literature review shows that several studies exist that investigate the various parameters of the Tesla valve. Nobakht et al. (2013) carried out CFD simulations and studied flow behavior in various sections of the Tesla valve. The work showed that significant energy loss occurs at the Y-junction when the flow is in the reverse direction. Zhao et al. (2024) considered straight-through Tesla valves with blades. It was shown that the pressure loss increased with an increase in blade width, inclination and pitch. The computational work of Zhang et al. (2024) found that the pressure drop in the Tesla valve improved with an increase in valve width. However, the improvement became insignificant when the width was made too large. Khabarova et al. (2017) carried out experiments for fluid diode devices. They showed that the flow becomes unstable and transient when the Reynolds number is greater than 500. A few papers, in addition to fluid flow, study related processes of heat transfer or phase changes in the Tesla valve. For example, Han et al. (2024) examined the two-phase boiling flow in several microchannel geometries. The results showed that vapor backflow was reduced in the Tesla valve channel, which improved the flow boiling performance. Huang et al. (2024) performed flow and thermal analysis that showed the presence of numerous eddies at the entrance of the valve, which greatly influenced the heat transfer rate. A Tesla valve with a symmetric shape was studied by Liu and co-researchers (2022), and they proved that the Hagen number was proportional to the square of the Reynolds number at higher velocities. Jiang et al. (2025) investigated temperature and pressure oscillations to suggest design improvements in a Tesla valve. The study by Du et al. (2023) predicted fluid flow and heat transfer performance in a Tesla valve using an artificial neural network technique. The optimal designs from their work increased the thermal and hydraulic efficiencies by 27% and 78%, respectively. Apart from these papers, several others considered Tesla valve for different applications such as photovoltaic thermal process (Hai et al., 2024; Zhao et al., 2024), hydrogen production unit (Chen et al., 2025) and printed circuit heat exchanger (Chou et al., 2024) All the previously published papers indicate that the design of Tesla valve can significantly affect the flow structure, diodicity and other performance parameters. In this paper, we have studied the effect of geometric parameters of Tesla valve on transient velocity profiles, pressure drop and diodicity. To the authors' knowledge, no study exists that examines the influence of Tesla valve geometry on unsteady flow behavior. Based on the fluid flow analysis, suitable geometries are proposed that can result in higher values of diodicity.

**2. Methodology. -**

**2.1 Tesla valve geometry and computational domain. -** To examine flow behavior in a Tesla valve, a computational domain was constructed as shown in Figure I. The valve consists of an inlet, an intermediate section consisting of branched channels for two possible flow paths and an outlet. One branched region is straight, while the other is curved. The curvature of the curved channel is defined with the help of two angles, α and β, which are the angles made by the

end and beginning sections of the curved branch with the horizontal. The height of the channel is 0.3 mm, and the outer radius of the curved section is 0.75 mm.

**2.2 Boundary conditions and assumptions. -** The effect of geometry on flow patterns and pressure drop is studied by specifying the inlet either to the left edge or to the (inclined) right end. These two cases are termed 'forward' and 'reverse' flow, respectively. Velocity was specified at the inlet, and a pressure outlet boundary condition was used at the outlet. The other surfaces were defined as 'wall', where the no-slip condition was applied. The effect of body force/gravity was neglected. The fluid was assumed to be water, which is a Newtonian and an incompressible fluid. The fluid properties, such as density and viscosity, thus, were constant and equal to 998.2 kg/m3 and 0.001 kg/m.s, respectively.

**2.3 Grid generation. -** The domain was divided into small volumes of quadrilateral shape using a grid. The grid was refined in the portions where the variation in velocity was expected to be higher, such as near the walls and in the regions where the fluids from two branches mix. The grid size was sufficient to obtain reliable pressure drop and diodicity values. For example, the results of diodicity were compared for valve geometries with α = 45° and 60° at Re = 2000 for various grid sizes, as shown in Figure II. The difference in diodicity was found to be less than 1% when cells were greater than 25000 cells, indicating that the results are independent of the grid. The convergence criterion for normalized residuals of continuity and velocity components was 1 x $10^{-5}$.

**2.4 Governing equations and discretization. -** Since most microfluidic applications involve low velocities, the problem in most cases turns out to be that of laminar two-dimensional flow. The governing equations were the continuity and the momentum equations for 2D unsteady flow that were solved using the Ansys Fluent code.

$$\frac{\partial u}{\partial x}+\frac{\partial v}{\partial y}=0 \qquad (1)$$

$$\frac{\partial u}{\partial t}+u\frac{\partial u}{\partial x}+v\frac{\partial u}{\partial y}=-\frac{1}{\rho}\frac{\partial p}{\partial x}+\nu\left(\frac{\partial^2 u}{\partial x^2}+\frac{\partial^2 u}{\partial y^2}\right) \qquad (2)$$

$$\frac{\partial v}{\partial t}+u\frac{\partial v}{\partial x}+v\frac{\partial v}{\partial y}=-\frac{1}{\rho}\frac{\partial p}{\partial y}+\nu\left(\frac{\partial^2 v}{\partial x^2}+\frac{\partial^2 v}{\partial y^2}\right) \qquad (3)$$

In equations (1-3), u and v are velocity components in x- and y-directions, respectively, p is pressure, ρ is density, and ν is kinematic viscosity. The equations were discretized using the QUICK scheme, and the pressure-velocity coupling was achieved using the SIMPLEC algorithm. Reynolds numbers up to 2000 were considered, and values of α and β were varied from 15°-60° and 30°-75°, respectively. The Reynolds number is defined as:

$$Re=\frac{\rho v d_h}{\mu} \qquad (4)$$

Where $d_h$ is hydraulic diameter, which is equal to twice of channel height h and μ is absolute viscosity.

At higher Reynolds numbers, particularly in the case of 'reverse' flow, the solution did not converge under steady conditions, indicating that the flow was not perfectly laminar. The solution in such a situation was obtained in unsteady mode without addition of any turbulence model. The unsteady/transient simulations were carried out using a second-order implicit scheme with a time step of 0.002 ms.

The performance of the device is compared using diodicity Di, which is defined as:

$$Di=\frac{\Delta p_R}{\Delta p_F} \qquad (5)$$

A higher value of diodicity indicates that the device has better flow directional control and is desirable.

**2.5 Validation. -** To validate the computational findings of this study, comparisons were made with previously published experimental and numerical results. The diodicity for one of the geometries considered in this paper (α = 45°, β = 75°) was calculated at different Reynolds numbers and compared with the experimental and numerical results in a similar geometry by Gamboa et al. (2005). This comparison is shown in Figure III, which shows that the difference between the diodicity values is within 30%. Since the diodicity values are low, this difference was considered acceptable and confirms the reliability of the results presented in this paper.

## 3. Results and Discussion

### 3.1 Single valve analysis

**3.1.1 Effect of α on flow behavior in Tesla valve. -** The velocity profiles typically found in a single Tesla valve are shown in Figure IV. The geometry of the valve has an angle α equal to 45°, and flow profiles are shown at two different values of Reynolds numbers. In the case of forward flow, it is seen that the flow mostly takes place in the bottom straight section, and the diversion of fluid into the curved section/branch is minimal. Flow recirculation is observed at the point where the curved section begins, while in the remaining portion of this curved loop, the fluid moves with a low velocity. A small recirculation zone could be seen downstream at the exit of the curved section where the curved and straight sections of the channel reunite, causing flow separation and recirculation (Figures IVa and IVc). When the flow direction is reversed (Figures IVb and IVd), the inlet fluid stream divides into two portions, creating prominent vortex flow in both sections of the valve. As the two flow streams remix at the outlet section of the channel, a much larger recirculation region could again be observed. Comparison of Figures (IVa with IVc) and (IVb with IVd) shows the effect of increasing the Reynolds number. As expected, the flow recirculation in both the curved and exit sections increased and became stronger at a higher Reynolds number value of 2000. The effect of angle α on flow patterns is shown in Figure V. The shape of the valve appears to change from a blunt shape to a relatively streamlined shape as the value of α is increased. Thus, with α = 15°, the fluid in the bottom portion must take a sharp turn before exiting the curved loop, while at α = 60°, it exits the channel relatively smoothly, whether in forward or reverse flow directions. For a moderate angle (α = 30°), significant recirculation regions in the top as well as the bottom branch are observed in the reverse flow. This behavior is similar, as was noticed in Figure IVd for the case of α = 45°. The transient response of pressure drop for four different α (15o, 30o, 45o, 60o) values in forward and reverse flow is presented in Figure VI. The pressure drop values shown in this Figure are taken after some simulation time has elapsed, and a fluctuating but repetitive or constant behavior in property variation is nearly obtained. The plots show that the flow is steady in the forward direction with all the angles considered. However, in the reverse direction, the flow is unsteady, except when α = 60°. The pressure required in reverse flow is found sufficiently larger than the pressure required for forward flow. The quantitative analysis based on time-averaged pressure drop shows that the diodicity [the ratio of pressure drop in reverse flow ($\Delta p_R$) to the pressure drop in forward flow ($\Delta p_F$)] is maximum when α is 45°.

**3.1.2 Effect of β on flow behavior in Tesla valve. -** The effect of variation of β, defined as the angle of inclination of the left portion of the curved section, is also studied when α is kept constant at 45°. As illustrated in Figure VII, for forward flow, an increase of β results in a slightly increased flow recirculation at the entrance of the curved section. In other regions, the velocity profiles are almost the same. In the case of reverse flow, at higher values of β (such as 60° or 75°), the forward fluid motion in the bottom section faces considerable resistance from the returning fluid flowing in the curved section. This leads to the formation of a major stagnant zone in which the velocity magnitude is nearly zero (Figures VIIf and VIIh). The pressure drop variation with time for different values of β is shown in Figure VIII. Like in the previous cases, in which the effect of angle α was discussed, the flow is steady in forward flow, whereas it is unsteady when the flow is reversed. The pressure drop remains between 6000-7000 Pa, showing an insignificant effect of β in forward flow. In reverse flow, the pressure drop is greater than 10,000 Pa for all the geometries, with much significant pressure drops for β = 60° or 75°.

**3.1.3 Pressure drop, diodicity and mass flow distribution. -** A comparison of the time-averaged pressure drop and diodicity values obtained for the different valve geometries considered in this study is given in Table I. The results show that when α is 15°, in forward flow, the pressure drop is higher than the other valves. This results in the lowest diodicity values with this valve at both the Reynolds numbers. Among the four tested valve geometries (while fixing β = 8.5), the geometry with α equal to 45° leads to maximum diodicity. The variation of β from 30°-75° while keeping α

= 45°, indicates that there is no appreciable change in pressure drop for forward flow. However, for reverse flow, the pressure drops are higher for large β angles. The comparison provided in Table 1 shows that valve geometry with α = 45° and β = 60° has maximum diodicity and is considered as the most suitable design among the tested valve shapes. The influence of geometry on mass flow in the two sections of the valve is also determined. The mass flow in the bottom (straight) and the top (curved) sections is represented by $m_1$ and $m_2$, respectively. The bar plot in Figure IXa shows that the mass flow rate in the top section is less than 10% of the inlet flow in forward flow. In addition, the mass flow rate in the top section ($m_2$) decreases with an increase in Reynolds number, indicating that the fluid entry into the curved section is further reduced at higher flow velocities. The ratio of mass flow also depends on the valve geometry, and it is noticed that increasing α increases the $m_2/m_1$ ratio. This is due to the streamlined shape at higher values of α, which allows more fluid to move through the top curved section. The $m_2/m_1$ ratios are also found to be low for different values of β during forward flow. As seen in Figure IXb, this ratio remains in the range 0.04-0.07 at Re = 1000 and between 0.02-0.05 at Re = 2000. In the reverse flow, the fluid entry to the curved section is fairly smooth, which allows sufficient mass of the fluid to move through this section. Thus, for reverse flow, $m_2/m_1$ is mostly greater than 1.

**3.1.4 Transient flow features. -** As observed earlier in Figures VI and VIII in terms of pressure drop, the flow in the forward direction is steady, while the flow in the reverse direction is usually transient at Re = 2000. The flow patterns in a Tesla valve are now discussed in further detail with the help of instantaneous velocity contours. The contours shown in Figure X are for the valve which has maximum diodicity. The results show that in the outlet section, the high velocity zone not only changes in magnitude but also in size and shape. This zone appears to be of extended size at one instant (for example, at 0.2 or 0.8 ms) and is found to split into multiple zones at other instants (0.6 and 1.2 ms). The changes that occur in the high velocity region lead to the movement of low velocity flow recirculation regions formed near the top and bottom walls of the outlet section.

The instantaneous flow structures can also be explained by tracking the velocity changes in time at specified locations in different sections of the valve. It is observed in Figure XI that at points ‘A’ and ‘B’, which are placed in the outlet section, the variation in velocity is significant. At point A, the x-velocity remains negative, which means the flow is moving towards the outlet section (towards the left). On the other hand, at point B, the x-velocity is positive, which indicates that flow recirculation is taking place at this point. At points ‘C’ and ‘D’, the fluctuation in velocity is small, showing that the flow is steady in the top and bottom sections.

**3.2 Performance of multi-stage valves. -** To further increase the system’s performance, multiple valves can be connected in series. Thus, the flow behavior in the valve, which has maximum diodicity (α = 45°, β = 60°), is examined with two and three stages. It is found from the time-averaged velocity profiles (not shown here) that the locations of high and low velocity regions are the same and repeat in different stages. The unsteady behavior, however, significantly changes as the number of stages is increased. A comparison is made in Figure XII in terms of the root mean square (RMS) values of velocity variation in time for the two and three-stage Tesla valves. The contour plots of Figure XIIa show that for the forward flow with two stages, the flow is steady. For a three-stage valve, near the exit section of the third stage, the velocity is found to vary considerably, showing flow unsteadiness. In reverse flow, the flow is unsteady in both the two-stage and the three-stage Tesla valves. In a two-stage valve, unsteadiness is more in the second stage when compared with the first stage, whereas in a three-stage valve, unsteadiness is more prominent in the exit section of the third stage and a common region formed by the second stage exit and the third stage inlet. The results thus show that the flow is steady in the beginning but becomes transient as it travels a certain distance inside the valve.

The flow instabilities in a multistage Tesla valve may also be attributed to the varying mass flow rates in the straight and curved sections of the valve. The mass flow rate is calculated at different time intervals in the straight and curved sections of the three-stage valve, and its variation is plotted in Figure XIII. A comparison of mass flow in the straight sections A, C and E shows that the mass flow rate at A has less variation, showcasing the flow’s quasi-steady nature, while at location C, the variation increased, but its value remained negative, indicating that the flow is still in the reverse direction. However, at location E, which lies in the third stage, the mass flow rate turned positive for a portion of the time interval and remained negative for the rest of the interval. This shows that the flow direction is continuously reversing in the straight section of the third stage. Since the total flow rate is constant, an increase in flow in the straight

section decreases flow in the curved section. Like the straight section, the flow rate is less fluctuating in the first stage and more fluctuating in the third stage. The diodicity for two and three-stage valves is calculated and summarized in Table II. The results show that for both Reynolds numbers, the diodicity increases with the increase in the number of stages. The number of stages can therefore be adjusted, based on the pressure/mass flow rate requirements in practical applications.

**4. Conclusions. -** The numerical work presented in this paper examines the fluid flow, pressure drop, diodicity and mass flow distribution in Tesla valves for Reynolds numbers up to 2000. When flow is in the forward direction, the fluid mostly takes a straight path, and less than 10% of the total inlet flow enters the curved section. In the reverse direction, a significant amount of fluid moves in the curved section. The ratio of mass flow rates in the two sections, for reverse flow, varies from 0.3 to 2.2, depending on the Tesla valve angles. The mixing of the fluid stream in a curved section with the stream in a straight section at the exit junction is often abrupt. This causes increased pressure drop, particularly in reverse flow. The effect of variation of angle α shows that for small angles (e.g., α = 15°), the fluid takes sharp turns, thus resulting in increased pressure drop in reverse as well as forward flow. On the other hand, when α is large, such as 60°, the streamlined shape of the valve reduces pressure loss in both forward and reverse directions. The diodicity values are therefore lower when α = 15° and 60°. For β = 8.5°, the valve with α = 45° results in maximum diodicity. The variation of β indicates that an increase in this angle does not affect the pressure drop in forward flow. In reverse flow, however, its larger values are found to increase pressure drop and hence diodicity. Multiple stages for the Tesla valve are considered, and flow patterns are examined in various stages. It is noticed that, though the time-averaged velocities are the same in different stages, the unsteadiness in flow is increased in the latter stages. The present work performs fluid flow analysis of the Tesla valve and examines its performance in terms of pressure drop/diodicity. Future work, in addition to fluid dynamics, will include the study of the Tesla valve for systems involving other phenomena such as heat transfer and phase changes.

**List of Symbols**

| | |
|---|---|
| dh | hydraulic diameter (m) |
| Di | Diodicity (-) |
| h | height (m) |
| $m_1$ | mass flow rate in bottom/straight section (kg/s) |
| $m_2$ | mass flow rate in top/curved section (kg/s) |
| p | pressure (Pa) |
| $\Delta p_F$ | pressure drop in forward direction (Pa) |
| $\Delta p_R$ | pressure drop in reverse direction (Pa) |
| Re | Reynolds number (-) |
| t | time (s) |
| u | x-component of velocity (m/s) |
| v | y-component of velocity (m/s) |
| x | horizontal / x-direction (m) |
| y | vertical / y-direction (m) |
| α | angle made by the left portion of the curved branch with the horizontal (°) |
| β | angle made by the right portion of the curved branch with the horizontal (°) |
| μ | viscosity (kg/m.s) |
| ν | kinematic viscosity (m2/s) |
| ρ | density (kg/m3) |

**Acknowledgement:** The authors acknowledge support provided by NED University of Engineering and Technology, Karachi for this work.

**Data Availability Statement:** The paper includes findings from CFD simulations performed on the commercial code Ansys Fluent. The simulation files are available from the authors. The description of the Tesla valve can be found in the patent (U.S. Patent 1329559A). The details of the code/software are available in software Ansys Fluent user guide.

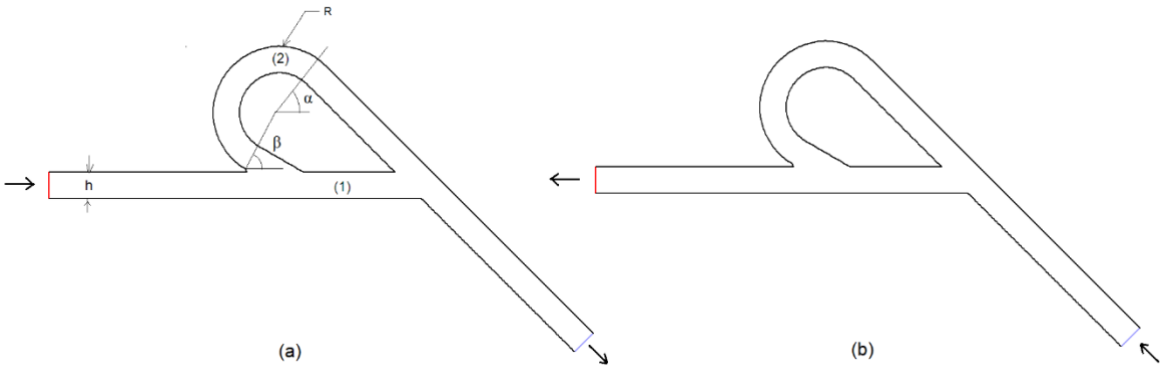


*Figure I. Geometry of Tesla valve considered with (a) forward (b) reverse direction*

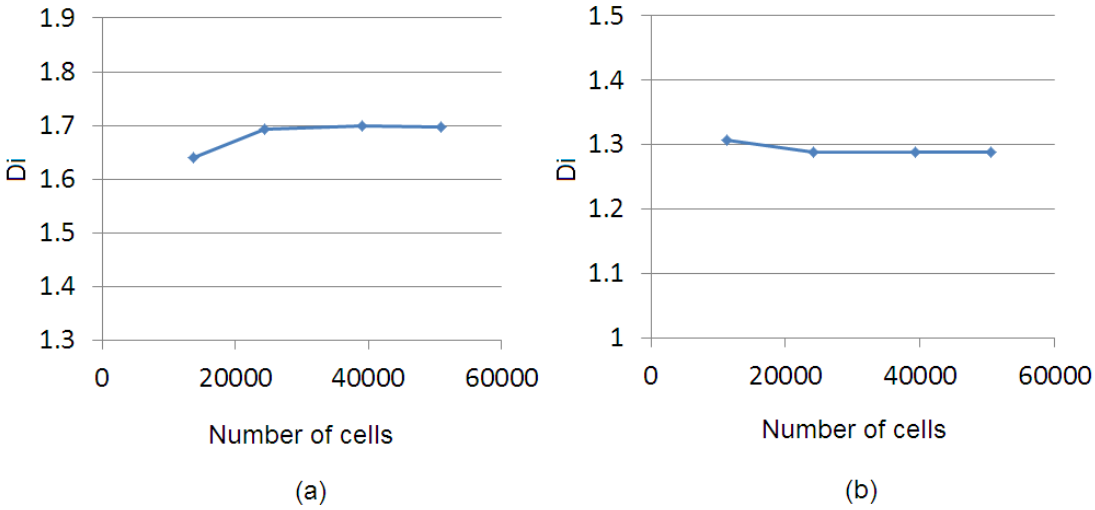


*Figure II. Diodicity versus number of cells (a) α = 45° (b) α = 60°, β = 8.5°, Re = 2000.*

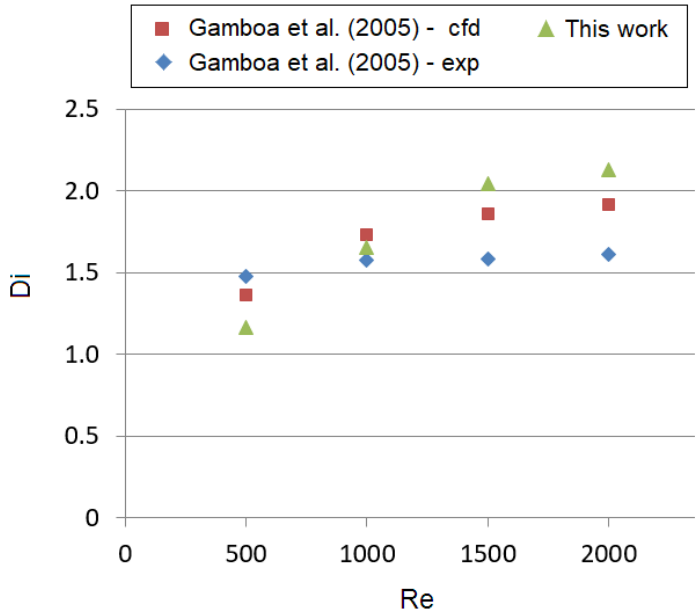


*Figure III. Comparison of present CFD results with previous literature (α = 45°, β = 75°)*

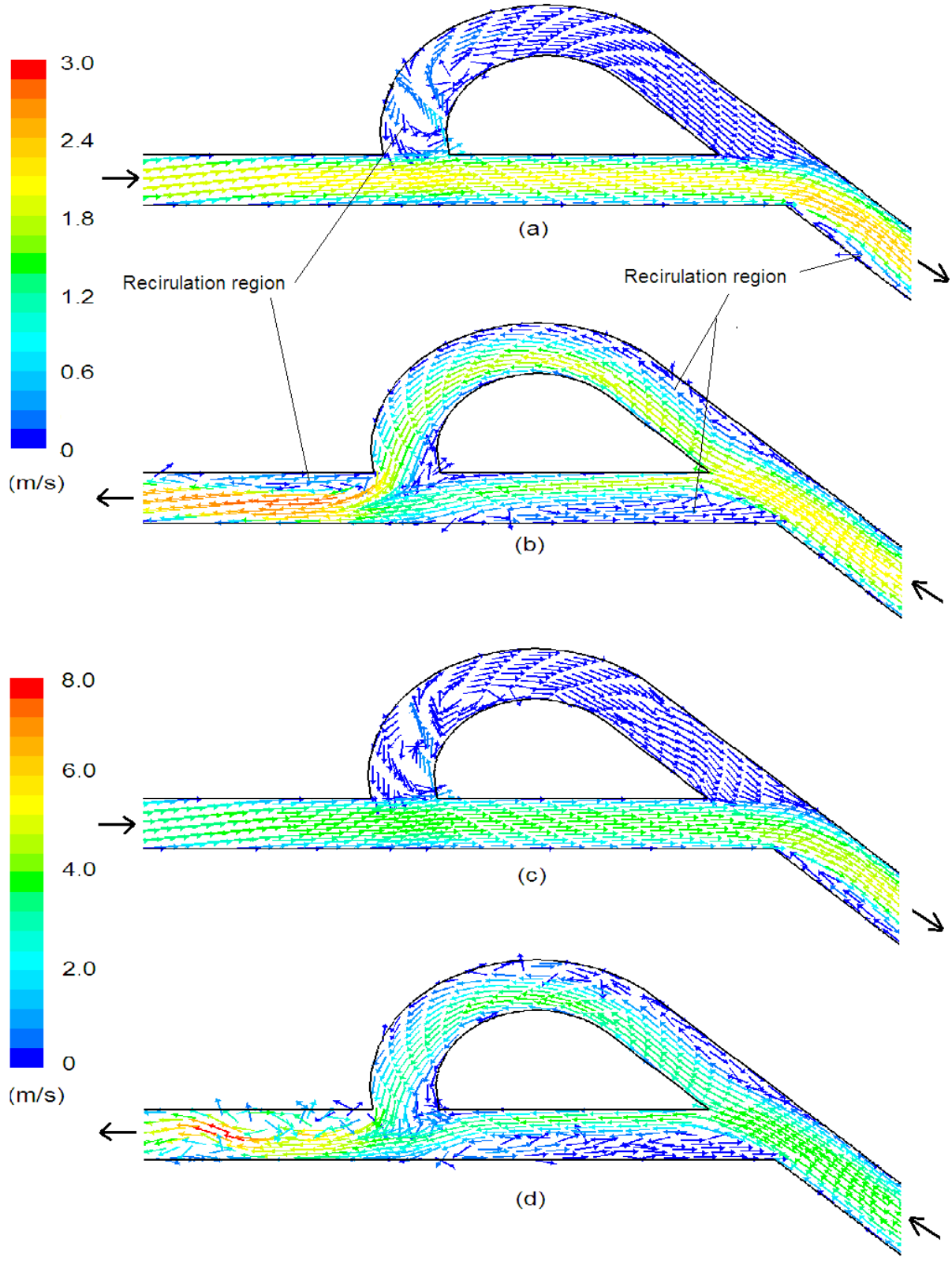


*Figure IV. Flow pattern in Tesla valve α = 45°, β = 8.5° (a) Re = 1000, forward flow (b) Re = 1000, reverse flow (c) Re = 2000, forward flow (d) Re = 2000, reverse flow*

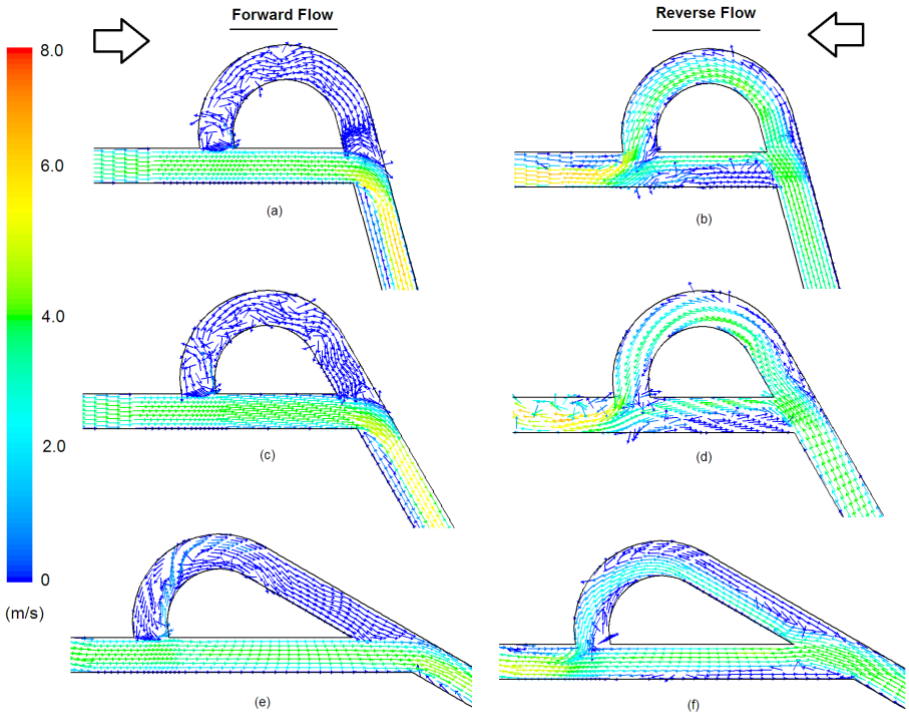


*Figure V. Velocity Vectors in Tesla valve (a) α = 15°, forward flow (b) α = 15°, reverse flow (c) α = 30°, forward flow (d) α = 30°, reverse flow (e) α = 60°, forward flow (f) α = 60°, reverse flow (Re = 2000, β = 8.5°).*

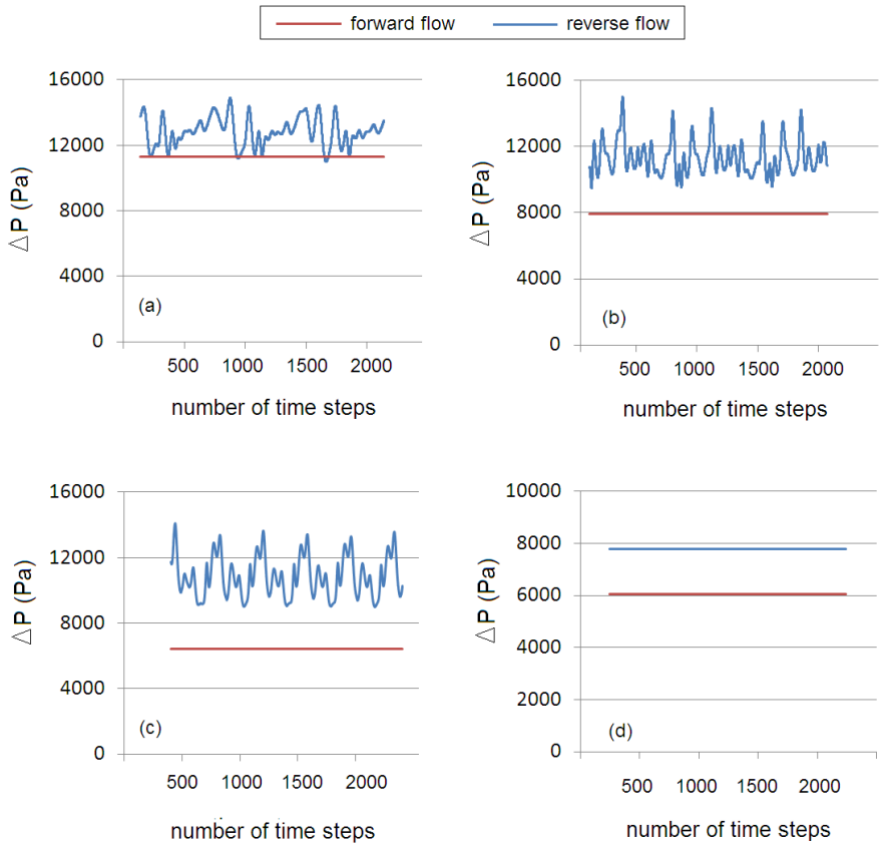


*Figure VI. Pressure drop with forward and reverse flow in Tesla valve (a) α = 15° (b) α = 30° (c) α = 45° (d) α = 60° (Re = 2000, β = 8.5°).*

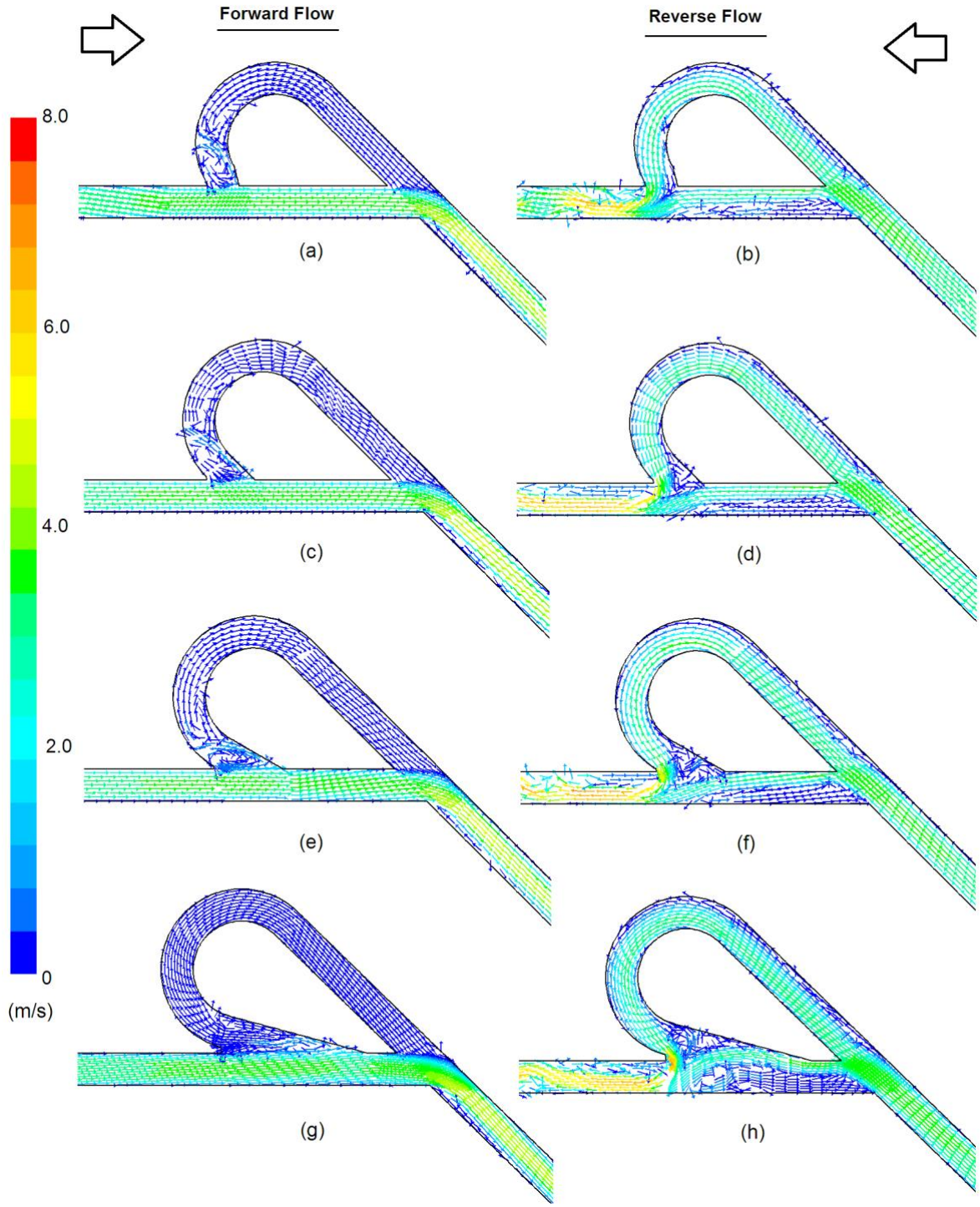


*Figure VII Flow pattern in Tesla valve (a) β = 30°, forward flow (b) β = 30°, reverse flow (c) β = 45°, forward flow (d) β = 45°, reverse flow (e) β = 60°, forward flow (f) β = 60°, reverse flow (g) β = 75°, forward flow (h) β = 75°, reverse flow (α = 45°, Re = 2000).*

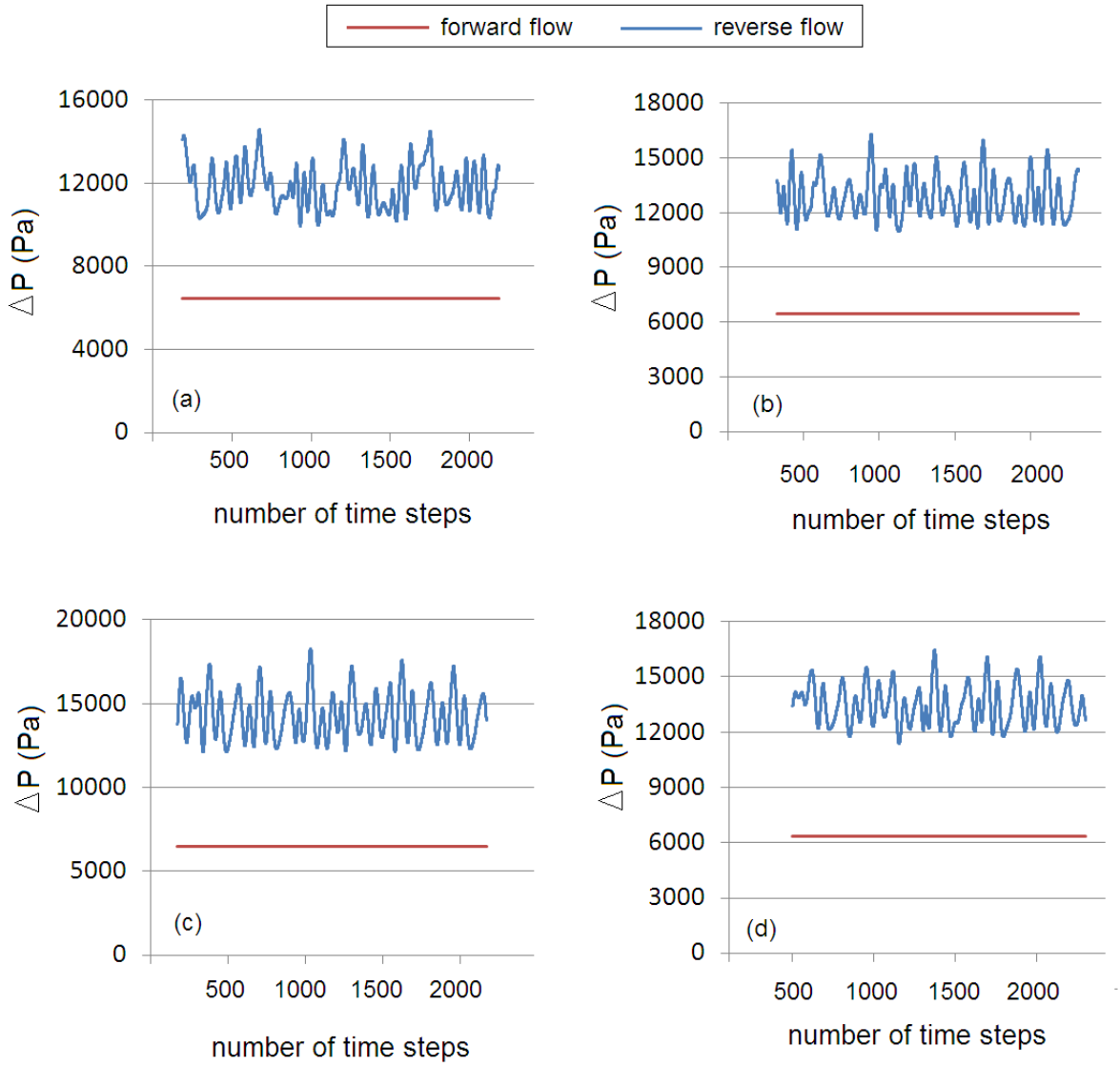


*Figure VIII* *Pressure drop with forward and reverse flow in Tesla valve (a) β = 30° (b) β = 45° (c) β = 60° (d) β = 75° (α = 45°, Re = 2000).*

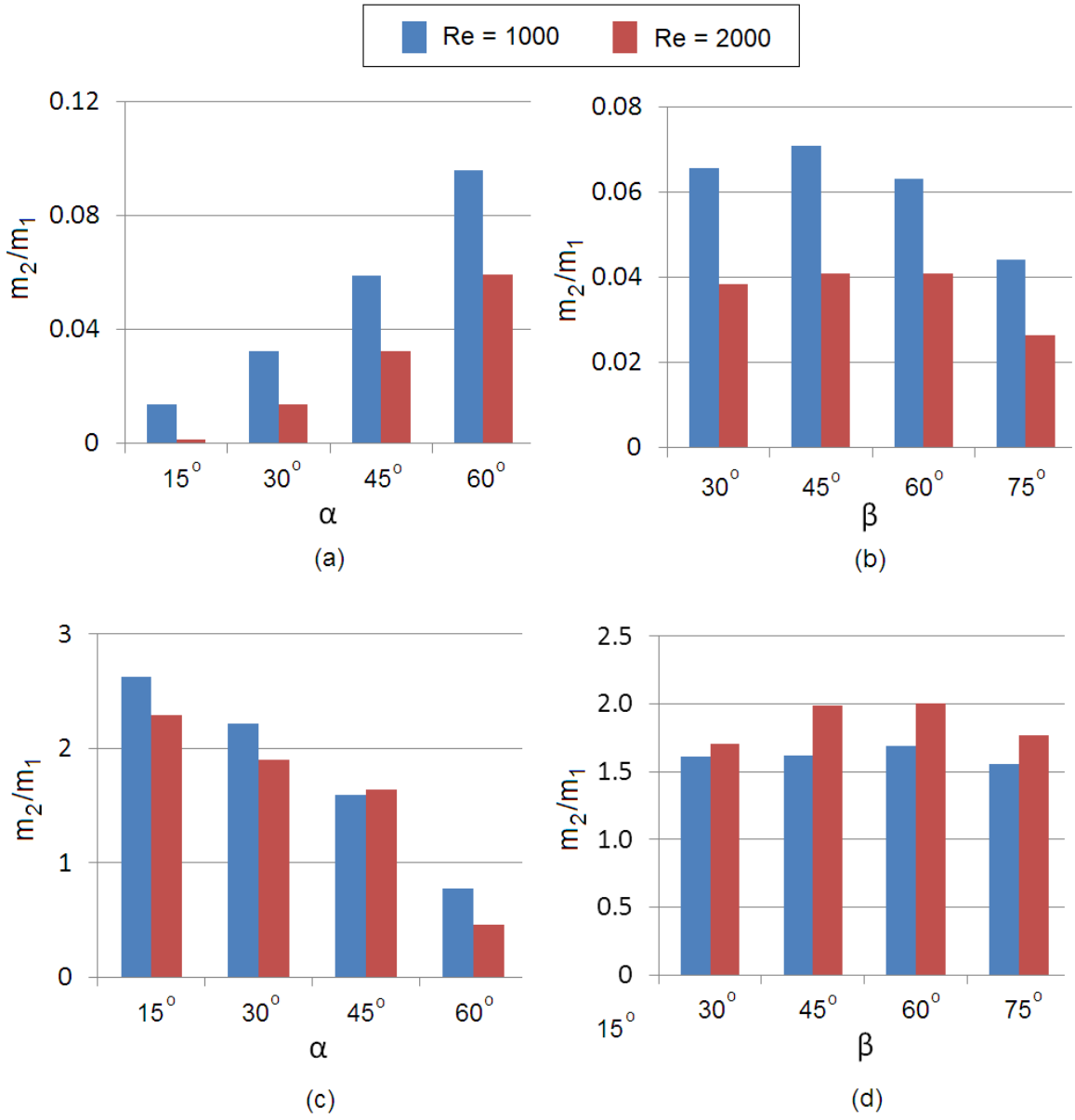


*Figure IX. Mass flow rate ratio versus (a) α, forward flow (b) β, forward flow (c) α, reverse flow (d) β, reverse flow (Re = 2000).*

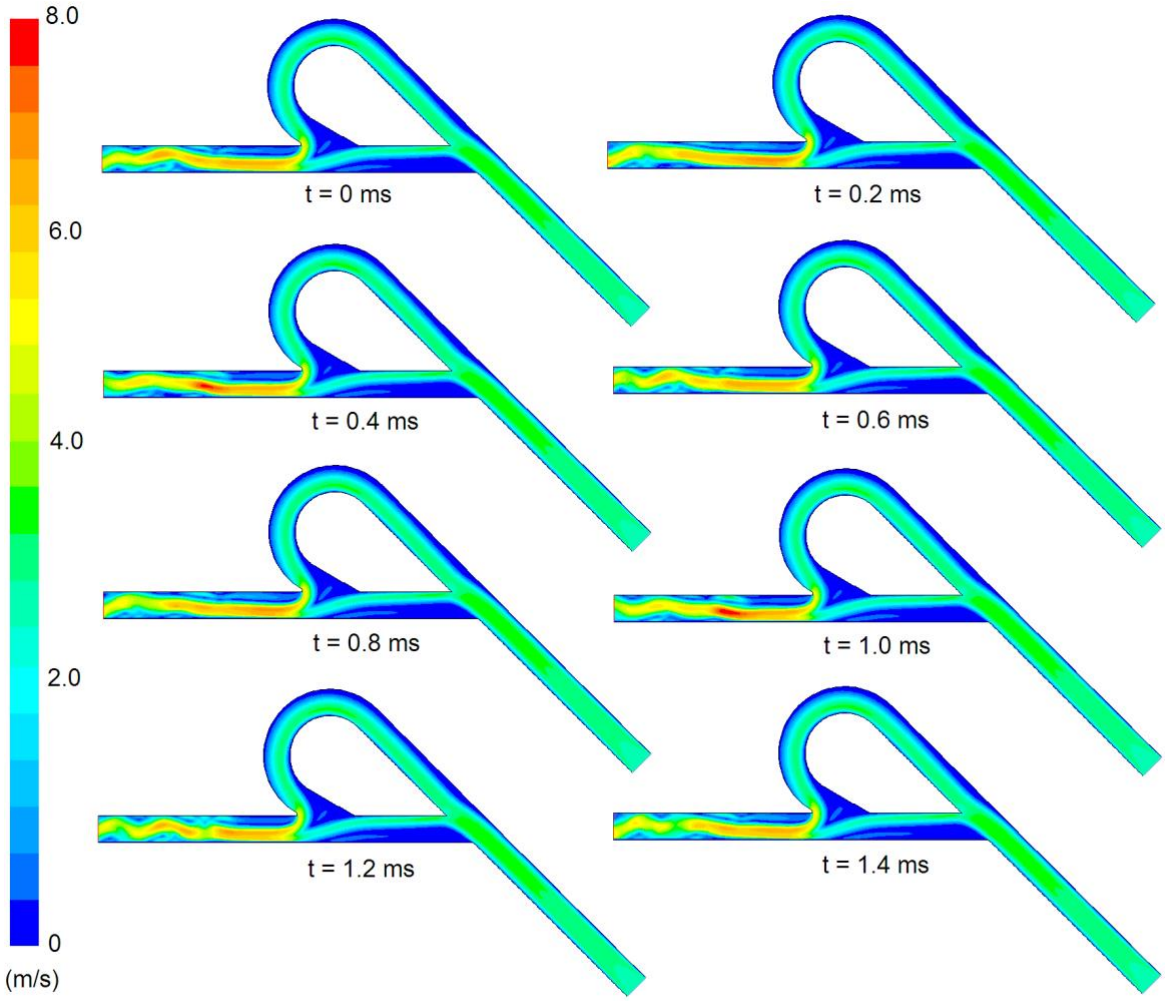


*Figure X. Unsteady velocity profiles in time at Re = 2000 (α = 45°, β = 60°).*

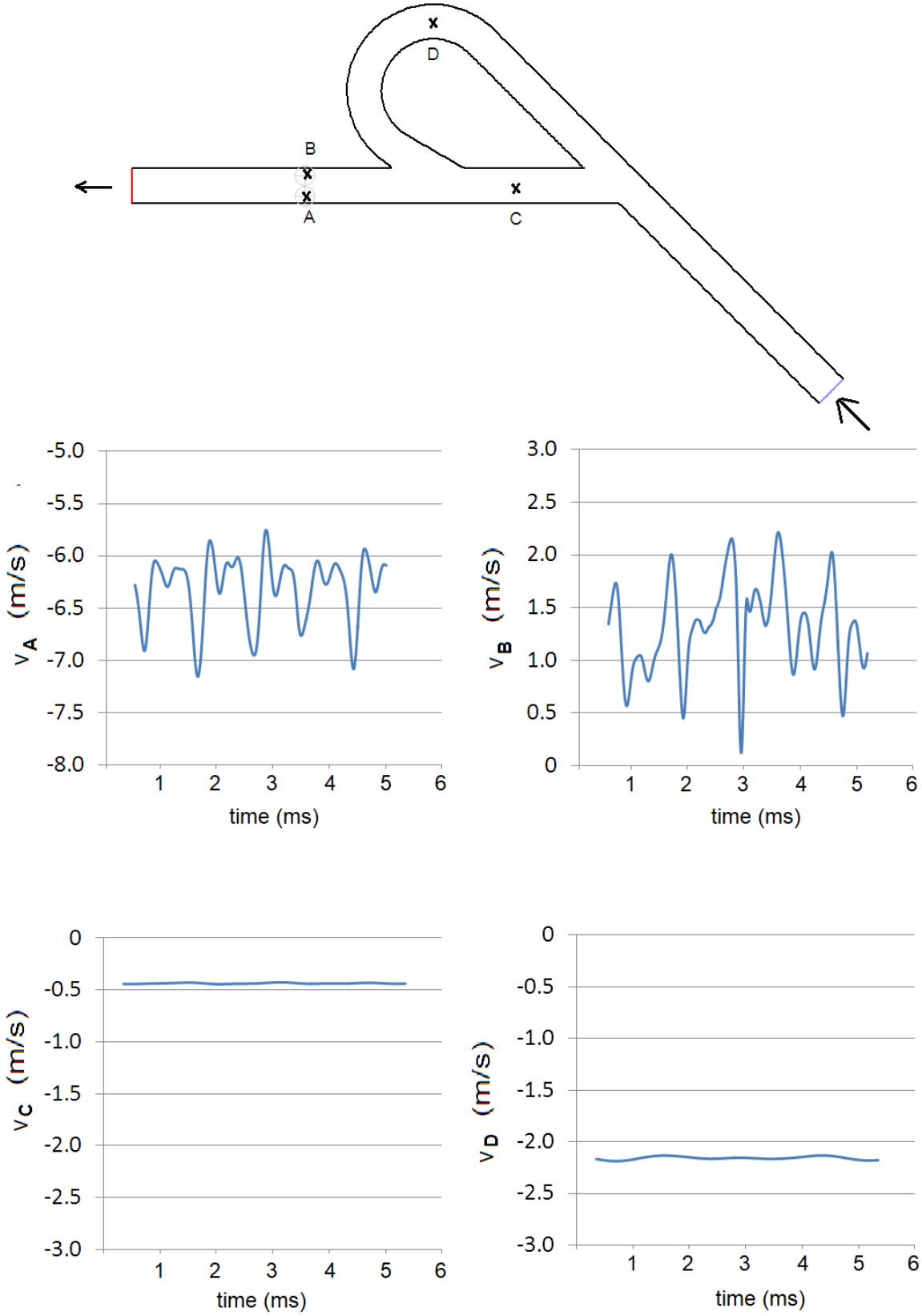


*Figure XI. x-velocity plot versus time at Re = 2000 (α = 45°, β = 60°).*

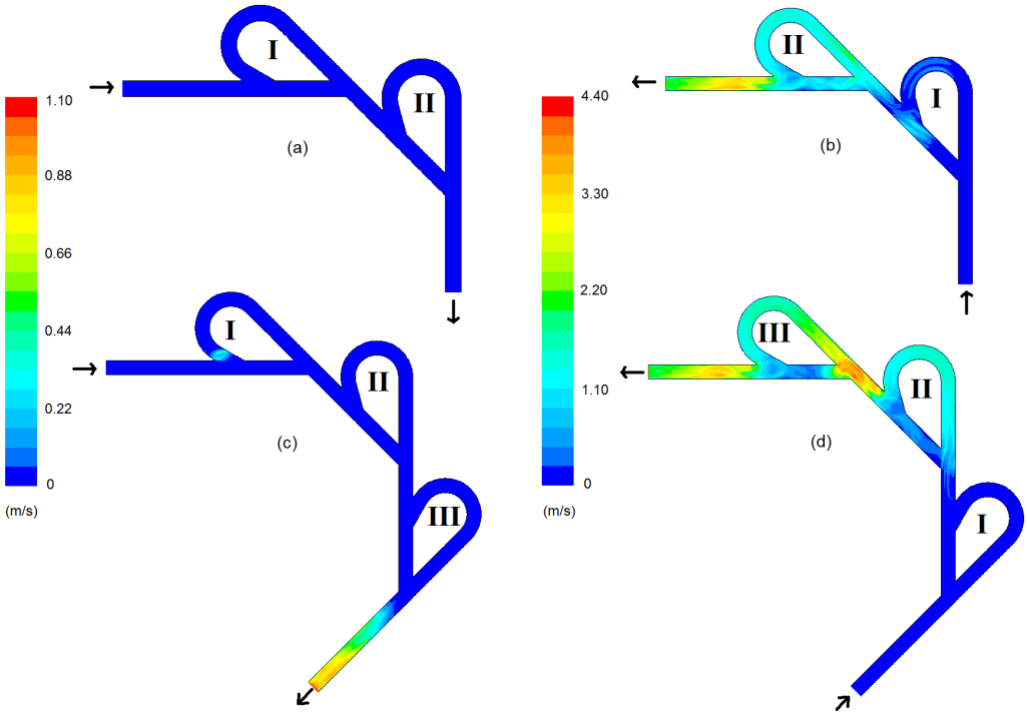


*Figure XII. RMS of velocity fluctuation in time (a) two stage valve, forward flow (b) two stage valve, reverse flow (c) three stage valve, forward flow (d) three stage valve, reverse flow (α = 45°, β = 60°, Re = 2000)*

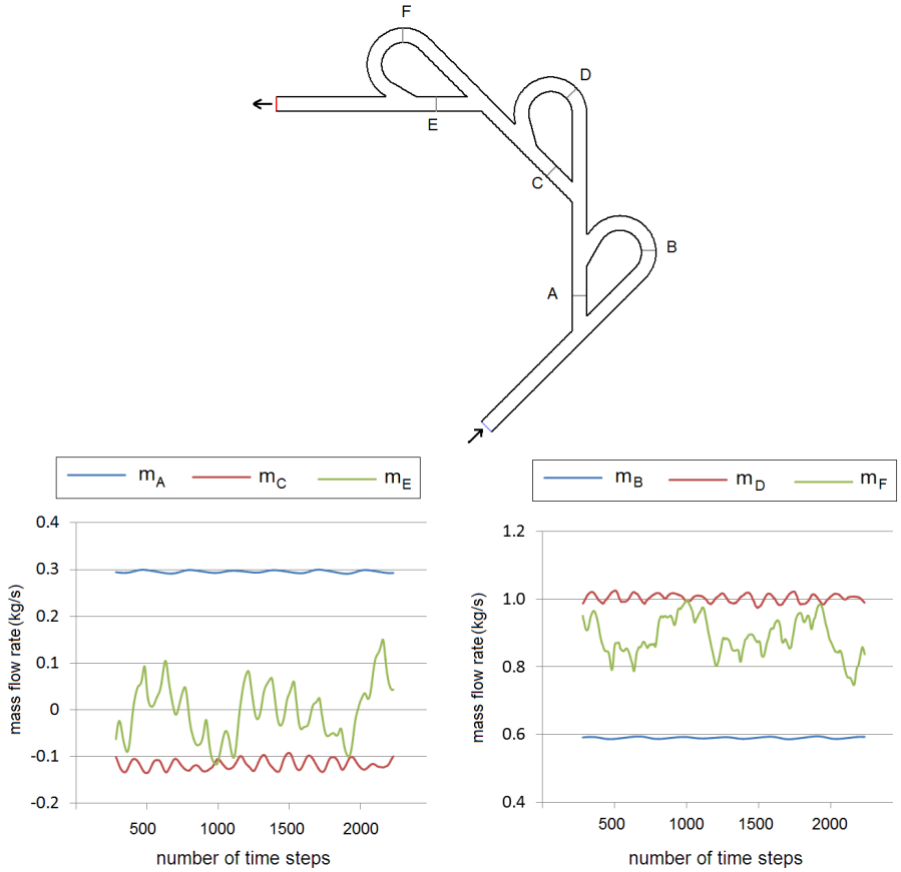


*Figure XIII. Mass flow rate variation at monitoring lines in straight sections (A,C and E) and curved sections (B,D and F), (α = 45°, β = 60°, Re = 2000)*

| | | *Re* = 1000 | | | *Re* = 2000 | | |
|---|---|---|---|---|---|---|---|
| $\alpha$ (°) | $\beta$ (°) | $\Delta p_F$ (Pa) | $\Delta p_R$ (Pa) | *Di* | $\Delta p_F$ (Pa) | $\Delta p_R$ (Pa) | *Di* |
| 15 | 8.5 | 2816.5 | 3419.7 | 1.21 | 11318.8 | 12856.5 | 1.14 |
| 30 | 8.5 | 2432.1 | 3353.1 | 1.38 | 7922.1 | 11343.2 | 1.43 |
| 45 | 8.5 | 2215.7 | 3114.0 | 1.41 | 6416.9 | 10864.4 | 1.69 |
| 60 | 8.5 | 2283.1 | 2786.6 | 1.22 | 6050.5 | 7797.9 | 1.29 |
| 45 | 30 | 2226.3 | 3371.3 | 1.51 | 6472.9 | 11857.5 | 1.83 |
| 45 | 45 | 2242.0 | 3550.3 | 1.58 | 6466.3 | 12878.6 | 1.99 |
| 45 | 60 | 2255.0 | 3807.6 | 1.69 | 6485.2 | 14248.5 | 2.20 |
| 45 | 75 | 2222.2 | 3677.5 | 1.65 | 6342.8 | 13485.8 | 2.13 |

*Table I. Effect of geometric parameters of Tesla valve on pressure drop and diodicity at Re = 1000 and 2000.*

| | **Two-stage valve** | | | **Three-stage valve** | | |
|---|---|---|---|---|---|---|
| *Re* | $\Delta p_F$ (Pa) | $\Delta p_R$ (Pa) | *Di* | $\Delta p_F$ (Pa) | $\Delta p_R$ (Pa) | *Di* |
| 1000 | 2938.1 | 9791.1 | 3.33 | 3750.4 | 15116.9 | 4.03 |
| 2000 | 9555.2 | 35384.3 | 3.70 | 12074.2 | 53653.9 | 4.44 |

*Table II. Pressure drop and diodicity for two and three-stage valves at Re =2000 (α = 45°, β= 60°)*

**References**

[1] Chen, M., & Li, Z. (2025). Conceptional design of passive system-level battery fire prevention device based on Tesla valve channel and phase change material. *Journal of Energy Storage*, *107*, Article e114942. https://doi.org/10.1016/j.est.2024.114942

[2] Chen, W.H., Zhing, M.H., Nguyen, T.B., Sharma, A.K., & Li, C.G. (2025). Hydrogen production in reverse tesla valve reactor combining ethanol steam reforming and water gas shift reaction. *Energy*, *318*, Article e134783. https://doi.org/10.1016/j.energy.2025.134783

[3] Chou, C.Y., Kuo, G.C., & Chueh, C.C. (2024). Numerical analysis of thermal-hydraulic influence of geometric flow baffles on multistage Tesla valves in printed circuit heat exchangers. *Applied Thermal Engineering*, *251*, Article e123601. https://doi.org/10.1016/j.applthermaleng.2024.123601

[4] Du, G., Alsenani, T.R., Kumar, J., Alkhalaf, S., Alkhalifah, T., Alturise, F., Almujibah, H., Znaidia, S., & Deifalla, A. (2023) Improving thermal and hydraulic performances through artificial neural networks: An optimization approach for Tesla valve geometrical parameters. *Case Studies in Thermal Engineering*, *52*, Article e103670. https://doi.org/10.1016/j.csite.2023.103670

[5] Gamboa, A.R., Morris, C.J., & Forster, F.K. (2005) Improvements in Fixed-Valve Micropump Performance Through Shape Optimization of Valves. *Journal of Fluids Engineering*, *127(2)*, 339–346. https://doi.org/10.1115/1.1891151

[6] Hai, T., Rahman, M.A., Aksoy, M., Zhou, J., Alenazi, M.J.F., Singh, N.S.S., Zain, J.M., & Jawawi, D.N.A. (2024). Investigating the performance of the Tesla valve channel in a photovoltaic thermal system through numerical simulation: Evaluation from the standpoint of thermodynamic laws. *International Communications in Heat and Mass Transfer*, *159*, Article e108197. https://doi.org/10.1016/j.icheatmasstransfer.2024.108197.

[7] Han, Q., Liu, Z., Yang, S., Han, J., Wang, Z., Miao, J., & Li, W. (2024). The role of Tesla valves in microchannel flow boiling. *International Journal of Heat and Mass Transfer*, *234*, Article e126148. https://doi.org/10.1016/j.ijheatmasstransfer.2024.126148

[8] Huang, F., Ren, L., Xie, S., Leng, M., & Liao, P (2024). Numerical study of flow characteristics and heat transfer mechanism in Tesla valve tube. *Results in Engineering*, *21*, Article e101795. https://doi.org/10.1016/j.rineng.2024.101795

[9] Jiang, E., Wang, W., Miao, J., & Zhang, H. (2025). Effect of the Tesla Valve on the heat transfer performance and the suppression of pressure drop oscillation in a liquid cooling loop. *International Journal of Thermal Sciences, 207*, Article e109356. https://doi.org/10.1016/j.ijthermalsci.2024.109356

[10] Khabarova, D.F, Podzerko, A.V., & Spiridonov, E.K. (2017). Experimental Investigation of Fluidic Diodes. *Procedia Engineering. 206*, 93–98. https://doi.org/10.1016/j.proeng.2017.10.443

[11] Liu, Z., Shao, W.Q., Sun, Y., & Sun, B.H. (2022). Scaling law of the one-direction flow characteristics of symmetric Tesla valve. *Engineering Applications of Computational Fluid Mechanics*, *16(1)*. 441–452. https://doi.org/10.1080/19942060.2021.2023648

[12] Nobakht, A.Y., Shahsavan, M., & Paykani, A. (2013). Numerical Study of Diodicity Mechanism in Different Tesla-Type Microvalves. *Journal of Applied Research and Technology*. *11(6)*, 876–885. https://doi.org/10.1016/S1665-6423(13)71594-3

[13] Purwidyantri, A., & Prabowo, B.A. (2023). Tesla Valve Microfluidics: The Rise of Forgotten Technology. *Chemosensors*, *11(4*), 256–277. https://doi.org/10.3390/ chemosensors11040256)

[14] Tesla, N. (1920). *Valvular Conduit* (U.S. Patent 1329559A, 3 February 1920) [Google Scholar]
Zhang, X., Cao, Z., Fang, K., & Yang, X. (2024). Study on the influence of different structural parameters on the performance of Tesla valve. *Journal of Physics*, *2707*, Article e012092, https://doi.org/10.1088/1742-6596/2707/1/012092

[15] Zhao, Y., Wang, R., Gao, D., Chen, H., & Zhang, H. (2024). Numerical investigation and optimization of a multi-stage Tesla-valve channel based photovoltaic/thermal module. *Renewable Energy*, *228*, Article e120573. https://doi.org/10.1016/j.renene.2024.120573

[16] Zhao, Y.J., Tong, J.B., Zhang, Y.L., Xu X.W., & Tong, L.H. (2024). Hydraulic loss experiment of straight-through Tesla valve in forward and reverse directions. *Science Progress, 107(3)* Article e39285767 https://doi.org/10.1177/00368504241269433.

**Author contribution:**

1. Conception and design of the study

2. Data acquisition

3. Data analysis

4. Discussion of the results

5. Writing of the manuscript

6. Approval of the last version of the manuscript

MS has contributed to: 1, 2, 3, 4.

MEuH has contributed to: 4, 5 and 6.

SMFH has contributed to: 5 and 6.

**Acceptance Note:** This article was approved by the journal editors Dr. Rafael Sotelo and Mag. Ing. Fernando A. Hernández Gobertti.